3D MODELING OF IRAN AND SURROUNDING AREAS FROM SIMULTANEOUS INVERSION OF MULTIPLE GEOPHYSICAL DATASETS

Charles J. Ammon[1], Monica Maceira[2], and Michael Cleveland[1]

Penn State[1] and Los Alamos National Laboratory[2]

Sponsored by the Air Force Research Laboratory[1] and the National Nuclear Security Administration[2]

Award Nos. FA8718-09-C-0007[1] and LA09-BAA09-12-NDD03[2]
Proposal No. BAA09-12

ABSTRACT

The objective of this work is to help improve seismic monitoring technology through the development and application of advanced multivariate inversion techniques to generate realistic, comprehensive, and high-resolution 3D models of the seismic structure of the crust and upper mantle that satisfy independent geophysical datasets. Our focus is on the region surrounding Iran from the east coast of the Mediterranean in the west, to Pakistan in the east, an area of prime importance to NEM, and a region with adequate calibration events to validate our model and to quantify its accuracy. Specifically, we are working to integrate surface-wave dispersion, receiver function, and satellite and ground-based gravity observations to help constrain the shallow seismic structure in the Arabian-Eurasian collision zone. Building on our earlier work combining receiver functions and surface wave dispersion, and surface-wave dispersion and gravity, we plan to continue to integrate geophysical data sets to create more broadly compatible earth models. We also explore geologically based smoothness constraints to help resolve sharp features in the underlying shallow 3D structure.

OBJECTIVES

The National Nuclear Security Administration (NNSA) and Air Force Research Laboratory (AFRL) have decided to investigate 3D modeling as part of the effort to improve knowledge of Earth's compressional and shear velocity structure. Such knowledge will help reduce uncertainty in our ability to accurately detect, locate, and identify small (mb < 3.5) seismic events, which in turn will lead to improved capabilities for nuclear explosion monitoring (NEM). For seismically active areas, with good ground-truth event coverage, earth models with limited accuracy can be corrected by interpolating results from nearby 'ground truth' events (using the kriging methodology) making it possible to detect, locate, and identify events even with limited resolution of Earth's structure. However, such approaches are less effective for smaller events, and event location and characterization remains a challenge for aseismic regions. To improve monitoring capability in such instances, we must develop better seismic earth models.

The objective of this work is to help improve seismic monitoring technology through the development and application of advanced multivariate inversion techniques to generate realistic, comprehensive, and high-resolution 3D models of the seismic structure of the crust and upper mantle that satisfy independent geophysical datasets. Our focus is on the region including and surrounding Iran (Figure 1) from the east coast of the Mediterranean in the west, to Pakistan in the east, an area of prime importance to NEM, and a region with adequate calibration events to validate our models and to quantify their accuracy.

Background

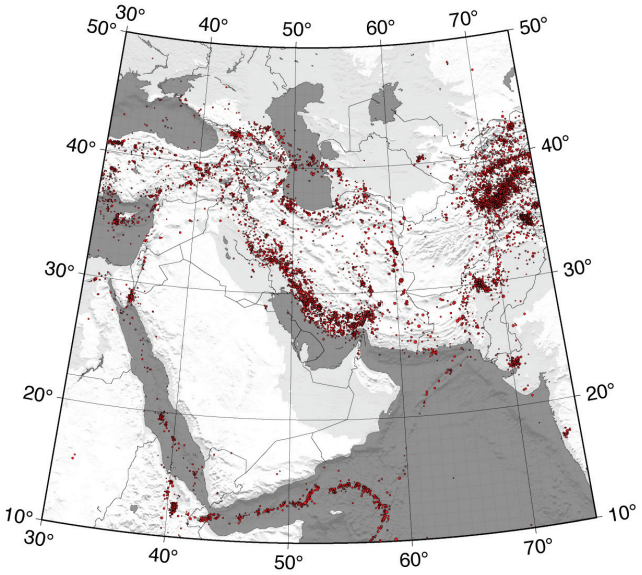

Figure 1 Map of focus region show with topographic and bathymetric shading and moderate to large earthquake locations (magnitudes ≥ 3.5 from 1990 to Spring 2008). The region contains the Arabian plate and the middle segment of the Alpine to Himalyan collision zone, which is constructed primarily of Phanerozoic terranes amalgamated onto southern Eurasia during the closing of the Tethys Ocean.

Estimating subsurface geologic variations is a challenge. Seismologists have worked on the problem for more than a century (e.g., Milne, 1899; Macelwane and Sohon, 1936; Dahlen and Tromp, 1999). As data quantity has increased and data quality and computational ability have improved, we have made important advances in our understanding of the subsurface. Our best knowledge applies to the shallowest regions as well as depths with the sharpest global interfaces (sediment-basement contacts, the base of the crust, base of the mantle, and transitions near 410 km and 660 km depths), where resolution is improved as a result of the strong interactions of seismic body waves with sharp geologic transitions (e.g., Helmberger, 1968; Langston, 1979; Shearer, 1991; Lay et al., 2004). We have also done well modeling regions with smooth velocity changes such as the lower mantle, which allows us to exploit the information in teleseismic body-wave travel times to locate seismic sources reasonably well (e.g., Kennett, 1991). Still, many details within and just beneath the lithosphere elude us. We have been able to surmise that geologic variations here are substantial, and we know that they frustrate attempts to use robust observations such as regional seismic travel times to locate events in many parts of the Earth (e.g., Bondar et al., 2004).

Travel-time based tomography (e.g., Nolet, 2008) opened the doors to 3D imaging but the models remain blurry, often suffer from interpretational ambiguity, and are not easily used to predict other, independent seismic observations. From our own analyses (Maceira et al., 2005; Maceira and Ammon, 2009), we have seen how high-resolution surface-wave tomography fails to produce the extremes in seismic shear-wave speed that are evident from independent observations. In particular, achieving a model with low enough seismic wave speeds within the Tarim Basin to match seismograms from high-quality observations remains an issue. Waveform tomography methods improve the situation somewhat, including information from both the amplitude and phase of the signal, but restriction of these methods to lower frequency bands limits the resolution of the methods and the substantial

computation requirements of these methods limit their application. More recent finite-frequency methods (e.g., Zhou et al., 2004; Dahlen and Zhou, 2006, Nolet, 2008) and adjoint methods (e.g., Tarantola, 1984; Tromp et al., 2008) offer more complete approaches to computing sensitivity kernels. But even these approaches face limits imposed by data bandwidth. In any event, such fully 3D waveform methods could benefit greatly from accurate, if approximate, starting models derived from more piecewise interpretation of seismic observables combined with other observations.

RESEARCH ACCOMPLISHED

Much of our effort during the first year of this project has been on the software development, although we have completed preliminary inversions that we present below with little discussion. At this point we caution readers about using or interpreting these preliminary earth models – they will improve. We begin with a simple conceptual illustration of the challenges we address and conclude with a discussion of accomplishments and plans for the second year of work.

Combining Gravity, Rayleigh-Wave Dispersion, and P-wave Receiver Function Observations

Inversion of surface wave dispersion observations is a standard method for estimating 3D shear velocity structure of Earth's crust and upper mantle. Nevertheless, it is well known that traditional state-of-the-art inversion techniques suffer from poor resolution and nonuniqueness, especially when a single surface-wave mode is used (Huang et al., 2003). This is particularly true at shallow depths where the shorter periods, which are primarily sensitive to upper crustal structures, are difficult to measure and especially true in tectonically and geologically complex areas. On the other hand, regional gravity inversions have the greatest resolving power at shallow depths since gravity anomalies decrease in amplitude and wavenumber bandwidth with increasing depth. Gravity measurements also supply constraints on rock density variations. Thus by combining surface-wave dispersion and gravity observations in a single inversion, we can obtain a self-consistent high-resolution 3D shear-velocity/density model with increased resolution of shallow geologic structures. Receiver function analysis (Langston, 1979) is a well-established tool for imaging relatively sharp changes in the subsurface structure that nicely complements information contained in surface-wave dispersion (e.g., Julià et al., 2000).

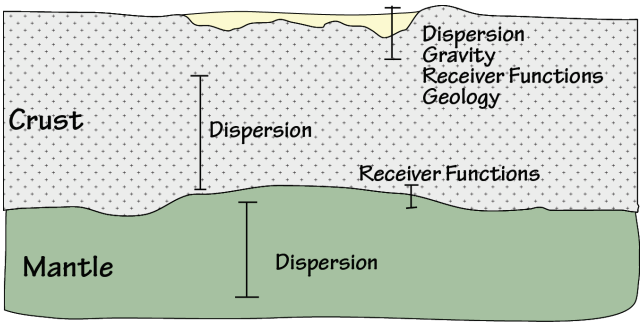

Figure 2 Conceptual illustration of the primary sensitivities of different data sets to the different depths of the lithosphere in a simultaneous inversion of surface-wave dispersion, gravity, and receiver-function observations. The crust shown contains a large basin (yellow). The receiver functions provide information on strong velocity contrasts such as the crust-mantle transition and near-surface structures; the spatially filtered gravity provides constraints on near-surface structures; and dispersion provides information on the absolute seismic velocities throughout the structure. Note that this cartoon is conceptual, the sensitivity of the data is more subtle than shown.

To improve our view of the earth structure within the focus region, we are working to combine receiver functions with surface-wave dispersion and gravity observations. The combination of receiver functions with tomographically localized surface-wave dispersion is well established (e.g., Julià et al. 2000). The integration of gravity observations with surface-wave dispersion is a more recent development (e.g., Maceira and Ammon, 2009), but these data are a good match. To a large part, the gravity observations add important constraints on the location of strong shallow heterogeneity to the information on smooth variations found in period-dependent dispersion maps. The choice of a density-velocity relationship can be subjective (Julià et al., 2004; Brocher, 2005; Maceira and Ammon, 2009), but testing the sensitivity of the results to a range of relations is not a challenge. To isolate gravity signatures associated with density variations (as opposed to dynamic and flexure variations) we plan to filter the gravity signals to include short wavenumbers sensitive to the crust. These concepts are summarized conceptually in Figure 2, which shows the regions of the lithosphere most sensitive to the different data that we employ.

To construct an approximate 3D model of the lithosphere, we use a hybrid 1D-3D inversion. In many tomography analyses, dispersion variations are converted to shear-velocity variations by inverting dispersion curves extracted from the tomographic model for a localized 1D structure. Smoothness constraints are applied to reduce cell-to-cell

shear-velocity fluctuations in the resulting composite 3D structure. Since gravity observations can be efficiently modeled using prisms they provide direct information on cell-to-cell density variations. In a particular cell, surface wave dispersion can be inverted simultaneously with receiver functions (surface or downward-continued signals). In regions with receiver function overlap, multiple signals can be combined to produce a structure that matches compatible features in several receiver functions. Because of the hybrid nature of the inversion, the resulting model is an approximation to the true 3D structure, but we can use to provide a starting point for future full 3D waveform-based inversions of the subsurface.

Preliminary Application to the Iranian Plateau and Surrounding Regions

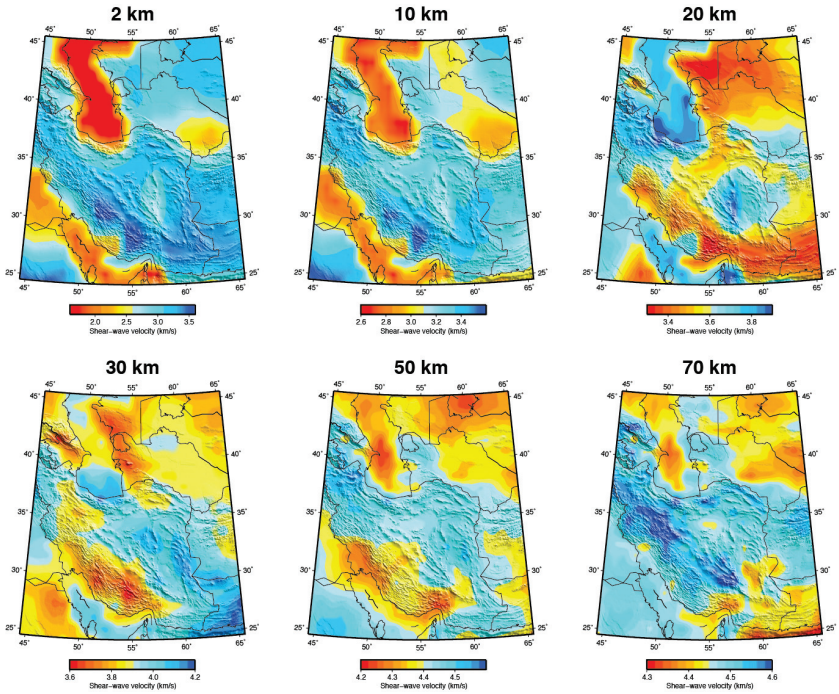

Figure 3. Results of a preliminary inversion of Rayleigh-wave dispersion and Bouguer gravity observations to estimate shear-velocity beneath the focus region. The inversion was performed using the existing SVD-based approach and took about 36 hours to compute on a high-end workstation. This result is preliminary and should not be used for specific interpretation. The extreme slow values for the shallow Caspian Sea are obvious; deeper values, particularly those with high wavenumbers are likely artifacts. The inversion weighted observations at shorter periods much more than longer-period observations.

A large component of the proposed work involves improving current software to allow more easy extension to larger focus areas and more flexible incorporation of additional data. For example, the earlier work in Maceira and Ammon (2009) blended gravity and surface-wave observations to produce a shear-velocity/density model for central Asia, but did not include receiver-function information. Our inversion is a straightforward composite of coupled and uncoupled linearized inversions of nonlinear data and model relationships. The preliminary results we present below do not have the gravity wavenumber filters applied. We rely on the dispersion models from the University of Colorado group (Ritzwoller and Levshin, 1998; Levshin et al., 2001, 2002) for the preliminary results, but we will include other measures as the project proceeds. Figure 3 is a plot of first-order shear-velocity variations beneath the study region. These are preliminary results, so we invest little space interpreting the variations. We started the inversion using only Rayleigh-wave dispersion in the period range from 7 to 200 seconds (with more weight on the shorter periods). Figure 4 shows example fits to the dispersion values and the Bouguer gravity variations. As seen in earlier studies (Maceira and Ammon, 2009) the addition of the gravity information produces little change to the overall fit of the dispersion values, but substantially improves the fit to the observed surface gravity signals.

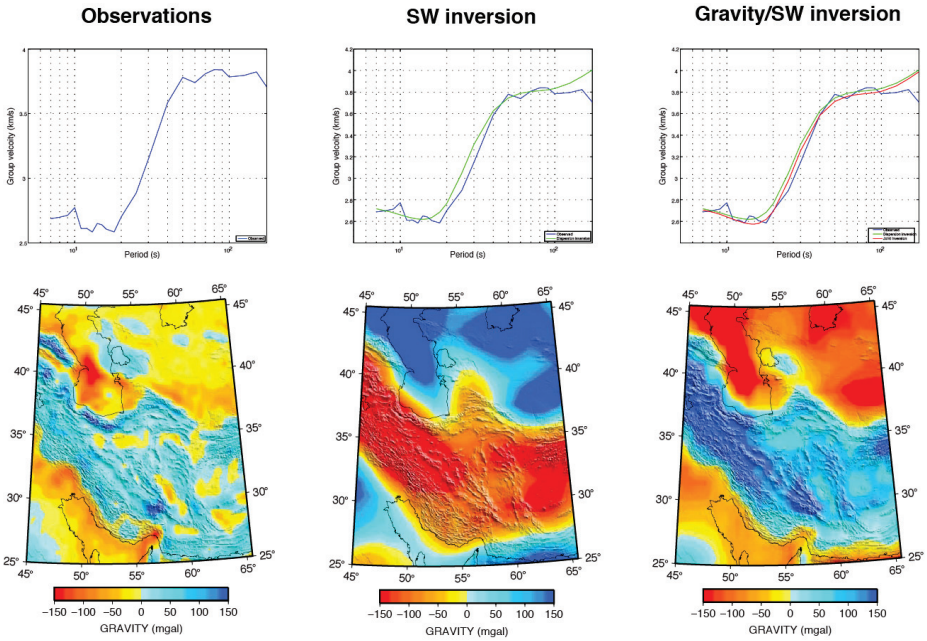

Figure 4. Sample dispersion (top) and Bouguer gravity (bottom) for the preliminary inversion. As for other regions (Maceira and Ammon, 2009), the inclusion of gravity observations produces a much better fit to the observed gravity variations with little change to the Rayleigh-wave fit. Note that the gravity in this inversion was not filtered to emphasize shorter wavelength variations in the gravity to focus on near-surface variations.

Software Development Progress

A large component of the proposed work involves improving current software to allow more easy extension to larger focus areas and more flexible incorporation of additional data. For example, the earlier work in Maceira and Ammon (2009) blended gravity and surface-wave observations to produce a shear-velocity/density model for central Asia, but did not include receiver function information. Our inversion is a straightforward composite of coupled and uncoupled linearized inversions of nonlinear data and model relationships. In essence we construct a large set of coupled data and constrain equations into the form $Gm = d$, where the model parameters are in m, observations and constraint information is in d, and the system matrix, G, contains partial derivatives and coefficients of constraint equations.

The existing inversion tool used a singular value decomposition (SVD) to invert the system matrix, G. The SVD is superb numerical choice for matrix inversion and problem analysis but the simplest implementations require substantial quantities of core memory and computational time as the problem grows large. To reduce these requirements we have replaced the SVD with Page and Saunders (1982) LSQR conjugate-gradient based routine. We adopted the LSQR function from the Association for Computing Machinery (ACM) FORTRAN implementation last modified in 1994 (http://toms.acm.org/). Although well known to seismic tomographers (Pavlis, 1988; Nolet, 1993), the benefits of the LSQR algorithm may be less familiar to those working on multi-dataset inversion tools. The key advantage is that the system matrix, G, need never be stored in memory. G can be stored on the disk as it is constructed one row at a time. The LSQR user need only develop a subroutine that computes $y = G\,y + y$ and $x = G^T x + x$, for vectors x and y provided during the inversion of G. G can be written to disk by saving only the nonzero columns of each row of the matrix and the associated indices of the nonzero columns. Not only do you save storage and input-output time, you also avoid waste by not multiplying numbers by zero. In our early experiments, we have saved roughly an order of magnitude in computation time (measured on a relatively simple desktop workstation). The great reduction in computation time allows more experimentation with and assessment of the model.

Example Rayleigh-Wave Dispersion Receiver Function Coupled Inversion

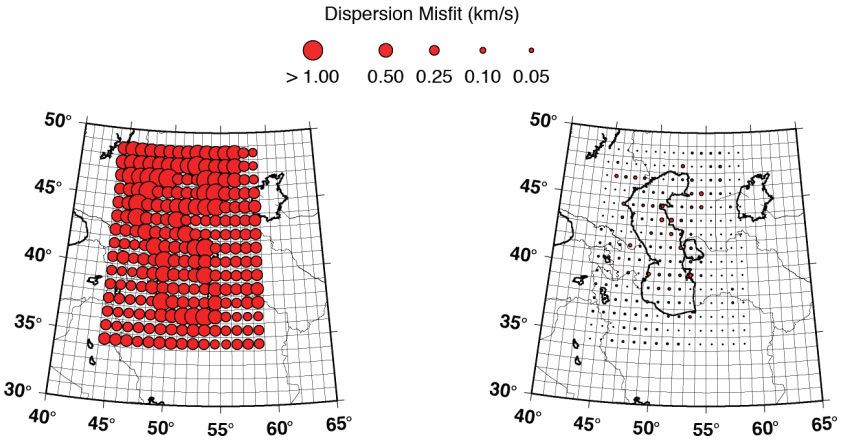

Figure 5. Initial (left) and final (right) dispersion misfit associated with the example subregion inversion of dispersion only. The initial model consists of a simple "continental" model and a Caspian Sea model. The initial misfits are large, but the convergence is reasonable to mean misfit values near or below 0.05 km/s.

To illustrate the result of combining surface-wave dispersion and receiver functions in a coupled inversion of cells for an approximation to a 3D model, we selected a small, but interesting region of the focus area that includes the Caspian Sea. The Caspian Sea region is an area of complex geologic structure (e.g., Mangino and Priestly, 1998) and significantly low shear velocities. The sub region is shown in Figure 5, which also shows the misfit to the dispersion values for each cell. As above, the dispersion values are from the University of Colorado tomographic effort (Ritzwoller and Levshin, 1998; Levshin et al., 2001, 2002). The initial misfits are large, but the inversion converges nicely to reasonable fits after four iterations (final). Two depth slices of the corresponding shear-velocity model (initial and final) are shown in Figure 6. The interpolation and contouring algorithm had some trouble with the rough initial model that contained two structures, one for region within the Caspian Sea and another for the rest of the model. We applied a simple Laplacian smoothing between adjacent cells so the resulting model remains smooth.

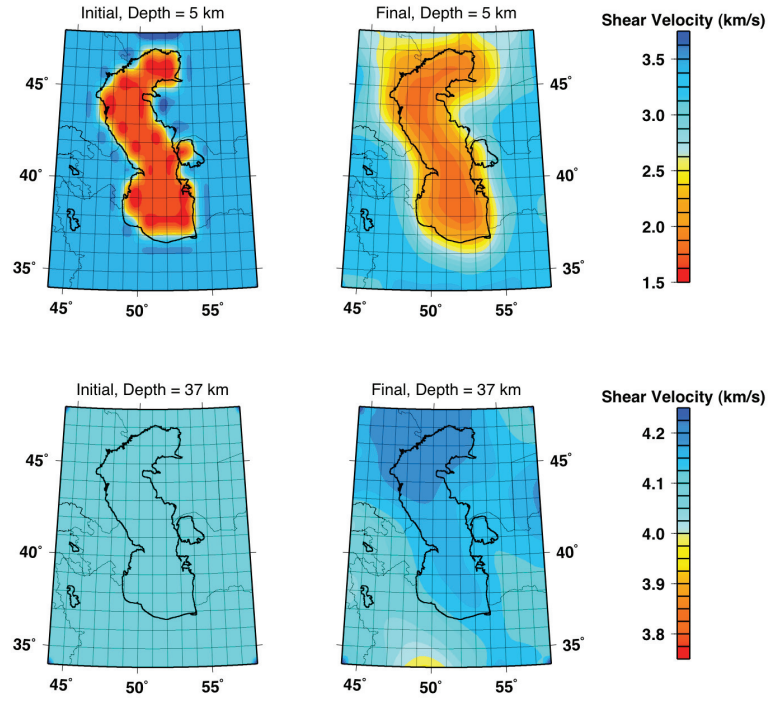

Figure 6. Initial (left) and final (right) shear-velocity values associated with the example subregion inversion of dispersion only for the upper and lower crust or upper mantle region of the model. The interpolation distorts the rough initial model producing artifacts that are absent when the inversion is complete and the model is smoother (we use a 1° cell dimension for the inversion).

Next, we added one receiver function to the dispersion data and repeated the 3D shear-velocity inversion. The receiver function was digitized from Mangino and Priestly (1998), and includes samples the structure in our cell with the lower left corner at 53E and 40N (Figure 7). Figure 7 is a plot of the initial and final dispersion fits, which show little change from those without the receiver function. The initial and final fit to the receiver function are shown in Figure 8. The effect of including the receiver function is to thicken the crust and better define the crust-mantle boundary. The net result is a decrease in the velocity at the depth slice near 37 km. Two depth slices of the corresponding shear-velocity model (initial and final) are shown in Figure 9. The thickening of the crust near the receiver function observation is clearly visible in the deeper slice through the model (compare Figure 6 and Figure 9). The fit to the receiver function is not perfect and the spread of the slower deep crustal speeds into the Caspian region does not make sense geologically.

These effects are driven by the simple Laplacian smoothness requirements placed on the 3D model.

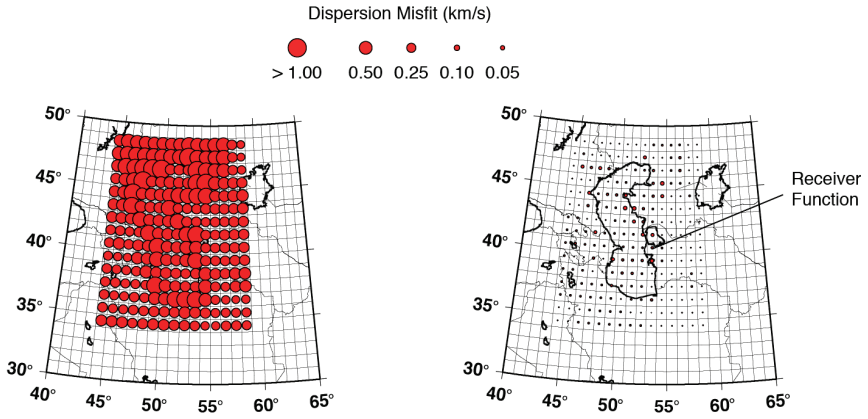

Figure 7. Initial (left) and final (right) dispersion misfit associated with the example subregion inversion of dispersion and a receiver function. The initial model consists of a simple "continental" model and a Caspian Sea model. The initial misfits are large, but the convergence is reasonable to mean misfit values near or below 0.05 km/s. The cell containing the isolated receiver function is labeled.

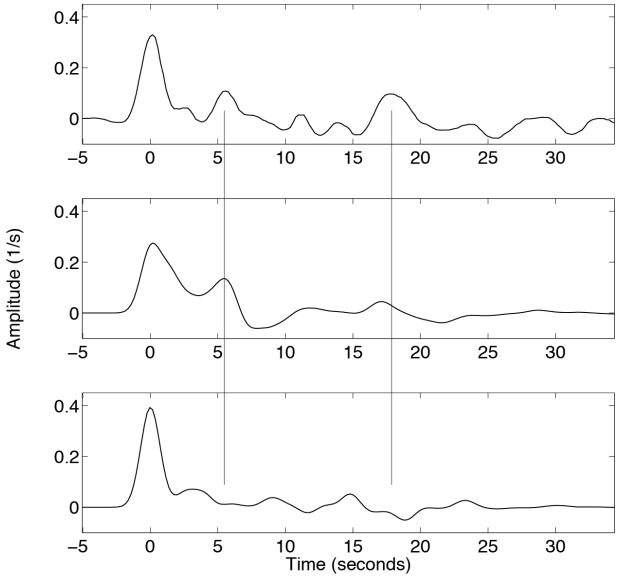

Figure 8. Observed (top), final prediction (middle) and initial prediction (bottom) of the receiver functions from the inversion shown in Figure 4. Vertical lines show the arrivals most likely associated with the crust-mantle transition. Although the final fit is certainly not perfect, note the improvement in timing of the main crustal conversion and reverberation (vertical lines) from the initial to final models.

Including Geologic Information

To produce models that have realistic 'sharp' boundaries requires that we include independent information on the location of those boundaries. Such information is available (for the shallow part of the model) in independent data sets such as gravity, surface geologic maps, and even something as simple as topography. As part of this work, we plan to resolve sharp features by adapting our imaging algorithms to allow the inclusion of geologic information on the location and nature of the boundary into shear-velocity inversions that permit such features (implemented through custom geologic smoothness constraints that allow velocities to be de-correlated across major geologic transitions). Including a priori information into an inversion is obviously only as good as the information that is included. Thus the inclusion of this type of information into the reconstruction of shear-velocity models of the

subsurface must proceed carefully and include documentation of the importance of the assumed a priori information on the resulting model.

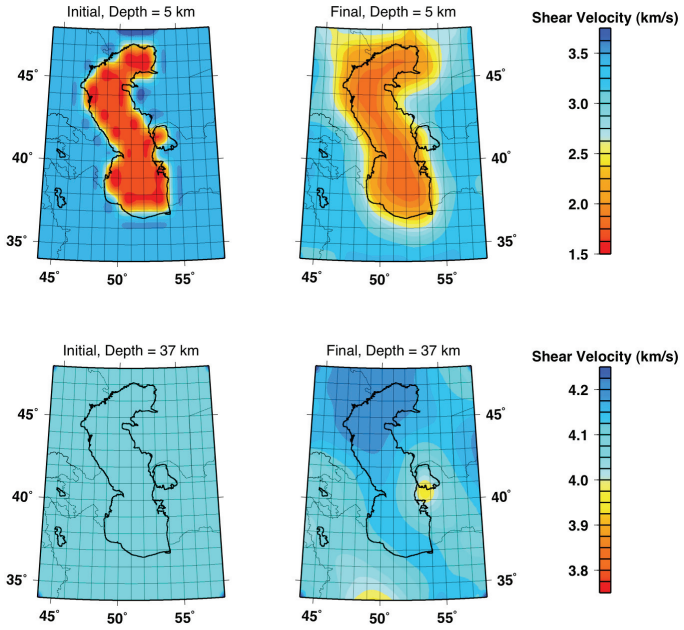

Figure 9. Initial (left) and final (right) interpolated shear-velocity values associated with the example subregion inversion of dispersion and a receiver function. The addition of the receiver function improves the estimate of crustal details. Please note the dramatic difference in the velocity scales shown to the right of each pair of images. The interpolation distorts the rough initial model producing artifacts that are absent when the inversion is complete and the model is smoother (we use a 1° cell dimension for the inversion).

We have made progress on including this type of information into the inversion, but have not finished debugging this component of the software. We expect that uncoupling the structures beneath a region of the Caspian Sea and its eastern margin will for example, allow a better fit to the KRF receiver function and decrease the leaking of receiver function model information into the model beneath the Caspian Sea. Implementation of these smoothing constraints requires more work, but in the end includes more information in the shear-velocity model reconstruction, and hopefully leads to improved regional earth models.

CONCLUSIONS

We have initiated a two-year project to map the subsurface geologic variations using seismic dispersion, gravity, and receiver-function observations. We face significant challenges in our efforts to include effective point constraints on structure (receiver functions) with the spatially continuous surface-wave tomography and gravity observations. Our work complements ongoing work at LANL to integrate body-wave travel times into the same formalism. The basic philosophy is that models that explain more data are better. The ultimate utility of the derived earth models is to provide improved predictive capabilities for routine seismic analyses and to provide adequate starting models for 3D waveform inversion approaches.

ACKNOWLEDGEMENTS

We thank the scientists, engineers, and technicians that have created the seismic-recording systems and networks that provide excellent broad-band seismic observations. In particular, we thank the USGS and the IRIS Consortia (NSF) who share information and data with the global community in an effective and efficient manner. We also thank the many international groups involved in collecting and sharing quality seismic observations. We also thank Wessel and Smith (1991), the developers of the Generic Mapping Tools software, which we use to create many of the illustrations of our research.

REFERENCES

Bondar, I., S. C. Myers, R. E. Engdahl, and E. A. Bergman (2004). Epicentre accuracy based on seismic network criteria, *Geophys. J. Int.* 156: 483–496.

Brocher, T. A. (2005). Empirical relations between elastic wavespeeds and density in the earth's crust, *Bull. Seismol. Soc. Am*. 95: (6), 2081–2092.

Dahlen, F. A. and J. Tromp (1999). *Theoretical Global Seismology*. Princeton University Press, Princeton, NJ, 1025 pp.

Dahlen, F. A. and Y. Zhou (2006). Surface-wave group-delay and attunuation kernels, *Geophys. J. Int*. 165: 545–554.

Helmberger, D. (1968). The crust-mantle transition in the Bering Sea, *Bull. Seismol. Soc. Am*. 58: 179–214.

Huang, Z., W. Su, Y. Peng, Y. Zheng, and H. Li (2003). Rayleigh wave tomography of China and adjacent regions, *J. Geophys. Res*. 108: doi:10.1029/2001JB001696.

Kennett, B. L. N. and E. R. Engdahl (1991). Traveltimes for global earthquake location and phase identification, *Geophys. J. Int*. 105: 429–465.

Langston, C. A. (1979). Structure under Mount Rainier, Washington, inferred from teleseismic body waves, *J. Geophys. Res.* 84: 4749–4762.

Lay, T., E. J. Garnero, and S. Russell (2004). Lateral variation of the D'' Discontinuity beneath the Cocos Plate, *Geophys. Res. Lett*. 31: L15612, doi:10.1029/2004GL020300.

Levshin, A. L., M. H. Ritzwoller, M. P. Barmin, and J. L. Stevens (2001). Short period group velocity measurements and maps in central Asia, in *Proceedings of the 23rd Seismic Research Review: Worldwide Monitoring of Nuclear Explosions*, LA-UR-01-4454, Vol. 1, pp. 258–269.

Levshin, A. L., J. L. Stevens, M. H. Ritzwoller, and D. A. Adams (2002). Short-period (7-s to 15-s) group velocity measurements and maps in central Asia, in *Proceedings of the 24th Seismic Research Review– Nuclear Explosion Monitoring: Innovation and Integration*, LA-UR-02-5048, Vol. 1, pp. 97–106.

Liang, C., X. Song, and J. Huang (2004). Tomographic inversion of Pn travel times in China, *J. Geophys. Res*. 109: B11304, doi:10.1029/2003JB002789.

Maceira, M. and C. J. Ammon (2009). Joint Inversion of Surface Wave Velocity and Gravity Observations and its Application to Central Asian Basins Shear Velocity Structure, *J. Geophys. Res.* 114: B02314, doi:10.1029/2007JB005157.

Maceira, M, S. R. Taylor, C. J. Ammon, and X. Yang (2005). High-resolution Rayleigh wave slowness tomography of central Asia, *J. Geophys. Res*. 110: doi:10.1029/2004JB003429.

Macelwane, J. B. and F. W. Sohon (1936). *Introduction to Theoretical Seismology, Part I, Geodynamics*. John Wiley and Sons, Inc., New York, 336 pp.

Mangino, S. and K. Priestley (1998). The crustal structure of the southern Caspian region, *Geophys. J. Inter*. 133: (3), 630–648.

Milne, J. (1899). *Earthquakes and Other Earth Movements* (4th Edition). D. Appleton and Company, New York, 376pp.

Nolet, G. (1993). Solving large linearized tomographic problems, in *Seismic Tomography - Theory and Practice*, edited by H. M. Iyer and K. Hirahara, pp. 227–247, Chapman & Hall, London.

Nolet, G. (2008). *A breviary of seismic tomography : imaging the interior of the earth and sun*, xiv, 344 p. pp., Cambridge University Press, Cambridge, UK; New York.

Pavlis, G. L. (1988). Vector and matrix manipulation algorithms, in *Seismological Algorithms, Computational Methods and Computer Programs*, edited by D. J. Doornbos, pp. 403–426, Acadmeic Press Limited, San Diego, CA.

Ritzwoller, M. H., and A. L. Levshin (1998), Eurasian surface wave tomography: Group velocities, *J. Geophys. Res*. 103: 4839–4878.

Shearer, P. M. (1991). Constraints on upper mantle dscontinuities from observations of long-period reflected and converted phases, *J. Geophys. Res*. 96: 18147–18182.

Tarantola, A. (1984). Inversion of seismic reflection data in the acoustic approximation, *Geophysics* 49: 1259–1266.

Tromp, J., D. Komatisch, and Q. Liu (2008). Spectral-element and adjoint methods in seismology, *Communications in Comp. Physics* 3: 1–32.

Wessel, P., and W. H. F. Smith (1991). Free software helps map and display data, *EOS, Trans. of Am. Geophys. Union,* 72: 441–445.

Zhou, Y. F. A. Dahlen, G. Nolet, and G. Laske (2004). Finite-frequency effects in global surface-wave tomography, *Geophys. J. Int*. 163: 1087–1111.